

UC Berkeley

UC Berkeley Previously Published Works

Title

Dynamic Energy Measurements in Charge Detection Mass Spectrometry Eliminate Adverse Effects of Ion-Ion Interactions.

Permalink

<https://escholarship.org/uc/item/6fd237fp>

Journal

Analytical Chemistry, 95(26)

Authors

Harper, Conner

Avadhani, Veena

Hanozin, Emeline

et al.

Publication Date

2023-07-04

DOI

10.1021/acs.analchem.3c01520

Peer reviewed



Published in final edited form as:

Anal Chem. 2023 July 04; 95(26): 10077–10086. doi:10.1021/acs.analchem.3c01520.

Dynamic Energy Measurements in Charge Detection Mass Spectrometry Eliminate Adverse Effects of Ion-Ion Interactions

Conner C. Harper,

Veena S. Avadhani,

Emeline Hanozin,

Zachary M. Miller,

Evan R. Williams*

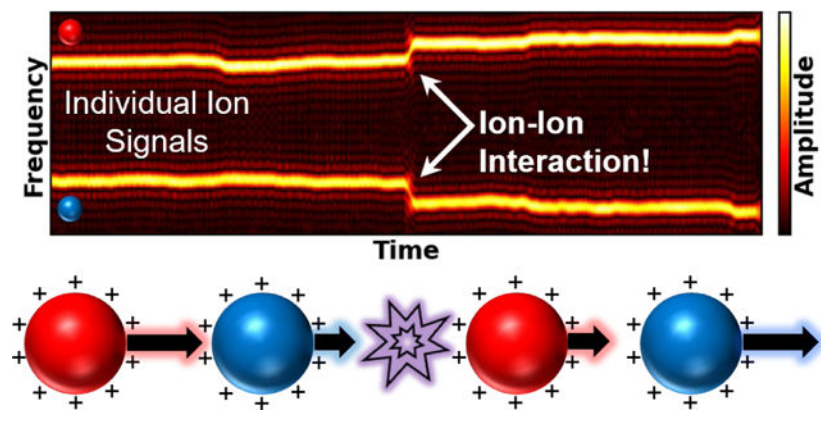
Department of Chemistry, University of California, Berkeley, California, 94720-1460, United States

Abstract

Ion-ion interactions in charge detection mass spectrometers that use electrostatic traps to measure masses of individual ions have not been reported previously, although ion trajectory simulations have shown that these types of interactions affect ion energies and thereby degrade measurement performance. Here, examples of interactions between simultaneously trapped ions that have masses ranging from ~2–350 MDa and ~100–1000 charges are studied in detail using a dynamic measurement method that makes it possible to track the evolution of the mass, charge, and energy of individual ions over their trapping lifetimes. Signals from ions that have similar oscillation frequencies can have overlapping spectral leakage artifacts that result in slightly increased uncertainties in the mass determination, but these effects can be mitigated by the careful choice of parameters used in the short-time Fourier transform analysis. Energy transfers between physically interacting ions are also observed and quantified with individual ion energy measurement resolution as high as ~950. The mass and charge of interacting ions do not change, and their corresponding measurement uncertainties are equivalent to ions that do not undergo physical interactions. Simultaneous trapping of multiple ions in CDMS can greatly decrease the acquisition time necessary to accumulate a statistically meaningful number of individual ion measurements. These results demonstrate that while ion-ion interactions can occur when multiple ions are trapped, they have negligible effects on mass accuracy when using the dynamic measurement method.

Graphical Abstract

*Address correspondence to this author. erw@berkeley.edu, Telephone: (510) 643-7161.



Introduction

Conventional mass spectrometry (MS) measurements require the formation and subsequent detection of a large number of gas-phase ions generated from a sample of interest. Coulombic repulsion between multiple ions with the same polarity can adversely affect MS measurements. MS methods in which ensembles of ions are trapped in a limited volume are especially susceptible to Coulombic effects. Often termed as ‘space charge’ effects, errors in the measured mass-to-charge ratios (m/z) due to ion-ion interactions have been observed and quantified in quadrupole ion trap MS,^{1–3} Fourier transform ion cyclotron resonance (FTICR) MS,^{4–7} and Orbitrap MS.^{8–11} In typical FTICR and Orbitrap experiments, coherent packets of ions with the same m/z are produced and oscillate at the same frequency to induce a signal on pickup electrodes.^{12,13} If the charge density of the packet is too high, Coulombic repulsion can lead to spatial dispersion of the ion packet. This reduces signal with time due to a loss of coherence and can lead to shifting ion frequencies and error in the m/z measurement.^{4–10}

A simple way to avoid any space charge effects is to trap only a single ion at a time. Experiments where only single ions or very few ions were trapped simultaneously have been performed using both FTICR^{14–16} and Orbitrap^{17–20} instruments. Compiling the measured m/z for many of these sparse ion trapping events results in improved resolution because space charge effects are essentially eliminated.¹⁸ Ion charge can be determined from changes in charge state of the individual ion,¹⁶ isotopic resolution or charge state resolution from the measurement of many individual ions,¹⁸ or from the amplitude of the single ion signal.^{19,20} In cases where the mass and/or heterogeneity of an analyte is sufficiently high such that charge states in m/z space can no longer be resolved and when charge is not lost during the measurement, then the charge must be obtained from the amplitude of the signal induced by each individual ion.^{19,20} In single ion Orbitrap measurements, the best demonstrated charge uncertainty from an amplitude-based measurement is ± 1 – 2 elementary charges (e) for ions trapped for 4096 ms.²¹ The inability to unambiguously determine charge from the signal amplitude is due in part to the dependence of ion signal on the ion orbital radius and the relatively high capacitance of the Orbitrap electrodes.²¹

Charge detection mass spectrometry (CDMS) instruments are expressly designed for high quality charge measurements of individual ions. Ions pass through cylindrical or other, similar ‘enclosing’ pickup electrode(s) and induce a current proportional to the ion charge that is not sensitive to ion position or velocity,^{22–25} enabling higher precision charge measurements than FTICR or Orbitrap-based methods. State-of-the-art CDMS instruments incorporate this detection electrode between the trapping electrodes of an electrostatic ion trap.^{26–29} In this configuration, the charges of individual ions can be resolved directly from signal amplitude measurements^{30,31} with a precision of $\pm 0.2 e$ demonstrated in a 1.5 s trapping period.³¹ The downstream electrode potential of the electrostatic ion trap is briefly lowered to let an ion beam pass through the detection electrode and is increased again to trap ions. This trapping and detection configuration means that ions are not ‘packetized’ (*i.e.*, ions with the same m/z having the same phase) as is done in FTICR and Orbitrap MS ensemble ion measurements. Instead, ions are spread throughout the trapping volume, significantly reducing the probability of ion-ion interactions. Similar to FTICR and Orbitrap MS, individual ion m/z is measured in CDMS based on the oscillation frequency of the trapped ions. The m/z of each individual ion is related to the oscillation frequency, f , via eq. 1,

$$\frac{m}{z} = \frac{C(E)}{f^2} \quad (1)$$

where $C(E)$ is a function of ion energy per charge and the electrostatic trap voltage and geometry.³² The charge of each individual ion is independently derived from the amplitudes of the fundamental and harmonic frequencies of the ion oscillation obtained from the Fourier transform (FT) of the time domain signal.^{30,32,33}

CDMS experiments where only a single ion is trapped at a time represent an ideal case for individual ion mass measurements on large and/or heterogeneous analytes for which charge state determination would otherwise be impossible.³⁴ However, measuring only a single ion at a time makes the accumulation of data for the many thousands of ions statistically required for meaningful characterization of a sample time consuming, generally requiring 30+ minutes.^{24,34} Multiplexed CDMS experiments where multiple ions are simultaneously trapped increase acquisition speed by more than an order of magnitude,^{35,36} but trapping multiple ions also introduces the possibility of ion-ion interactions. Simulations by Botamanenko and Jarrold suggest that ion-ion interactions will occur in CDMS when as few as two ions are simultaneously trapped, yielding shifting ion frequencies over time.³⁷ These authors also suggest that energy transfer between ions that occurs as a result of interactions will ultimately reduce the achievable resolution in m/z and mass measurements.³⁷ However, this conclusion is based on the assumption that the ion energy per charge (hereafter referred to as ion energy) and, therefore, the term $C(E)$ in eq. 1, are constant. This assumption of constant energy is based on the use of energy-filtering optics prior to detection, which has been used in many CDMS applications.^{24,34} In this case, any event that changes ion energy, including fragmentation, charge loss, solvent evaporation, and collisions with background gas in addition to ion-ion interactions, must result in reduced measurement accuracy.^{37,38}

An *in situ* method to dynamically measure the energies of individual ions using CDMS has been developed to address energy changes^{32,39} and has been used previously to characterize ion fragmentation,^{35,39} solvent evaporation,^{32,39–41} charge emission,^{40,41} and the relationship between energy lost to collisions and ion cross sections.^{32,42} However, ion-ion interactions have not previously been observed in CDMS experiments. In this work, multiple ions are simultaneously trapped for long time periods to maximize the probability of observing ion-ion interactions. Examples of ion-ion interactions over a broad mass and charge range are shown. The dynamic energy measurement method is used to quantify the effects of both signal-based interferences and physical ion-ion interactions on measurements of ion mass, charge, and energy.

Experimental

Charge Detection Mass Spectrometry.

Experiments were performed using custom-built CDMS instruments^{25,29,39} and signals were analyzed using methods that have been described in detail elsewhere.^{26,29,30,32,35} Briefly, ions are formed by nanoelectrospray ionization using borosilicate emitters with tip diameters of 1.5–5 μm . Ions travel through guiding ion optics and multiple stages of differential pumping until they reach an electrostatic conetrapp that contains a cylindrical detector electrode. Ions are trapped for a user-selected period of time (either 5 or 7.5 s in this work) and the signals induced on the detector are amplified by a charge-sensitive preamplifier (Amptek A250 CoolFET) and a custom bandpass filter stage with a gain of ~ 10 . Signals are digitized at 1 MHz and analyzed using a program that performs unapodized short-time Fourier transforms (STFT), picks and fits fundamental and harmonic peaks in each STFT segment, and uses frequencies and amplitudes of the fits to dynamically determine individual ion masses, charges, and energies.³⁰ A STFT with a segment length of 50 ms and step size of 5 ms was used in all experiments except where otherwise specified.

Materials.

Recombinant tobacco mosaic virus (TMV) was expressed and purified according to procedures described in previous work.^{30,43,44} TMV forms 17-mer disk-shaped structures (301 kDa) that can stack to form higher-order stacking oligomers. TMV samples were prepared at ~ 0.5 mg/mL in a 100 mM ammonium acetate solution. A sample of ~ 100 nm diameter NanosphereTM size standardized polystyrene nanoparticles (Thermo Scientific, catalog #: 3100/3100A, $\sim 1\%$ w/v aqueous suspension) was diluted by a factor of 500 into 0.5% aqueous acetic acid. A sample of ~ 45 nm surface amine-functionalized polystyrene sphere sample (2.5% w/v aqueous suspension) was obtained (Sigma Aldrich, product #: L0780) and diluted by a factor of 500 into 0.5% acetic acid.

Results and Discussion

Dynamic Energy Measurements

Multiple ions can be simultaneously trapped and analyzed in CDMS. Measuring multiple ions simultaneously is desirable because it significantly decreases the acquisition time required to compile a statistically robust mass distribution of the molecules in a sample.^{35,36}

Each trapped ion produces a periodic signal with a fundamental frequency of motion that can be extracted using Fourier transform analysis. To gain time-resolved information on the behavior of trapped ions, short time Fourier transform (STFT) analysis is commonly used in CDMS and in Orbitrap-based individual ion analysis.^{20,21,35,45} The STFT consists of the transformed data for short, successive segments of the time domain data and makes it possible to track ion properties as they evolve during the trapping period. Time-resolved measurements are important because ion masses, charges, and energies can change when ions undergo processes such as fragmentation,^{35,39} charge emission,^{40,41} solvent evaporation,^{32,39–41} collisions with background gas,^{32,39,42} and interactions with other ions. Well-defined ion energies are integral in the accurate measurement of both ion m/z (eq. 1) and charge.^{26,38} Therefore, changes in ion energy over the course of the trapping period limit the accuracy and precision of mass measurements if a singular ion energy is assumed, as is often done in CDMS experiments employing energy-filtering ion optics.^{24,34} However, the amplitudes of the fundamental ion oscillation frequency and associated harmonic frequencies in the Fourier transform of an ion signal make it possible to measure the energy as well as the charge and mass of each ion during each time segment of the STFT. These dynamic measurements for each individual ion can then be fit as a function of time to more accurately characterize ion properties even as they evolve over the trapping period.^{32,40}

Effects of Signal Interferences in Multiplexed CDMS

The evolution of the fundamental frequency of two out of six total simultaneously trapped tobacco mosaic virus (TMV) disk stack ions that were trapped for 7.5 s is shown in Figure 1, which will be referred to subsequently as a STFT plot and shows the frequency as a function of trap time. These two ions, while having the nearest frequency proximities relative to the other four trapped ions, are sufficiently well separated in the frequency domain such that their signals do not interfere and there is no evidence of physical ion-ion interactions. The frequencies of both ions increase by ~ 10 Hz/s over the trapping period, a phenomenon that has been observed elsewhere and attributed to energy losses due to solvent evaporation and collisions with background gas.^{32,40} For the ions with initial frequencies of 15,987 Hz and 16,330 Hz shown in Figure 1, linear fits of the measured energies in each segment yield initial ion energies of 206.0 ± 0.6 eV/ z and 202.1 ± 0.8 eV/ z and energy changes of -3.7 ± 0.9 eV/ z and -2.7 ± 1.1 eV/ z over the 7.5 s trapping period, respectively. Similar fits for the mass and charge for each ion do not indicate a significant change over the trapping period, meaning that the energy change observed can be largely attributed to collisions with background gas and not to solvent evaporation, charge emission, or fragmentation. Because no significant change in mass or charge is observed, these properties are simply averaged across all STFT segments. For the lower and higher frequency ions, respectively, the measured masses are 2.428 ± 0.008 MDa and 2.164 ± 0.007 MDa, and the measured charges are 106.0 ± 0.36 e and 97.7 ± 0.28 e . These masses and charges correspond well to stacks of 8 and 7 TMV disks, which have been observed previously for similar TMV samples.⁴³ These two ions represent the simplest case for multiplexed ion measurements; the ion signals do not interfere, there are no significant physical interactions during the trapping period, and the change in energy due to collisions with background gas can be straightforwardly tracked and accounted for, enabling a high accuracy measurement of mass and charge.

Because the uncertainty of the dynamic energy measurement method used to track individual ion energies in this work is based on the signal to noise ratios (S/N) of the amplitudes of the fundamental and harmonic frequencies, it improves with increased charge on the ion.²⁶ Figure 2a shows the STFT trace of a single ~100 nm diameter spherical polystyrene nanoparticle trapped for 5 s with a mass of 307.0 ± 0.6 MDa and a charge of $861.4 \pm 0.9 e$. The ion experiences a slight frequency shift over the course of the 5 s trapping period, starting at 4,742 Hz and ending at 4,761 Hz. As was the case for the TMV ions shown in Figure 1, this frequency shift is due to collisions with background gas that decrease the ion energy. The initial energy of this ion was determined to be 223.01 ± 0.24 eV/z. The energy resolution achieved for this ion is 945, which is a factor of ~3 times greater than the best energy resolution achieved to date with energy filtering optics in CDMS.³⁸ This enables high-precision mass measurements and demonstrates that a mass resolution of ~500 can be achieved using this method for ions in this mass and m/z (~350,000) range. The precision of the energy measurement also makes it possible to detect subtle changes in ion energy over the course of the trapping period. In this case, the ion energy changed by -0.79 ± 0.33 eV/z over the 5 s trapping period. This smaller change in eV/z compared to the TMV ions of Figure 1 despite the much larger physical size of the ~100 nm diameter nanoparticle is due to several factors, including the shorter trapping time, lower frequency, and the scaling of the total energy carried by the ion relative to the ion collisional cross section.

Due to the high charge of the 100 nm diameter nanoparticle, spectral leakage, or “ringing” artifacts, such as those highlighted in red in the single STFT segment (4000–4050 ms) shown in Figure 2b, are prominent. Spectral leakage occurs as a consequence of finite sampling of a waveform and depends on the choice of the apodization function. Previous work has shown that rectangular apodization, *i.e.*, no apodization, is most favorable for analyzing CDMS signals,^{30,36} although other apodization functions have also been used.²⁷ The characteristic peak shape of the rectangularly apodized FT is based on the sinc(x) function, which leads to spacing between ringing artifacts that is equal to $1/t$, where t is the length in time of the FT (in this case, the STFT segment length) and thus the 50 ms STFT segments used here give artifacts spaced by 20 Hz. Longer STFT segment lengths would reduce the frequency spacing of these spectral leakage artifacts and decrease potential interferences with other signals. However, the use of longer STFT segments necessarily comes at the cost of both decreased time resolution and a greater extent of frequency “smearing” that reduces amplitude measurement accuracy for signals that change in frequency.³⁶ Use of apodization functions is another way to reduce the prominence of spectral leakage artifacts, but at the cost of increasing peak width by a factor of ~2 or more.⁴⁶ Rectangular apodization is preferred in multiplexed CDMS measurements because peaks for ions that would otherwise catastrophically overlap and be misidentified or precluded from measurement can be resolved and weighed.^{30,36} Rectangular apodization in the FT also has the lowest equivalent noise bandwidth, which translates to the highest S/N and more accurate mass, charge, and energy measurements.³⁰ The use of super-resolution techniques, such as those based on the filter diagonalization method (FDM), could in theory be used to achieve sharper frequency peaks and eliminate spectral leakage artifacts as an alternative to STFT analysis.⁴⁷ However, these techniques are not as robust for the relatively low S/N individual ion signals acquired in CDMS experiments and are also significantly

more computationally demanding,^{47,48} making it difficult to achieve the real-time data processing currently implemented using STFTs.³⁰

Spectral leakage can become relevant when multiple highly charged ions are simultaneously trapped and ion signal peaks overlap with “ringing” artifacts generated by other nearby ion signals. An example of this phenomenon is shown in Figures 2c–d, where the signals of two ~100 nm diameter nanoparticle ions are separated by ~170 Hz. The measured masses and charges are 333.4 ± 1.3 MDa and 344.3 ± 1.0 MDa and 1069 ± 1.6 *e* and 971.4 ± 1.6 *e*, for the lower and higher frequency ions in Figure 2c, respectively. The initial energies of the lower and higher frequency ions were 249.76 ± 0.38 eV/*z* and 224.23 ± 0.31 eV/*z* and changed by -1.60 ± 0.54 eV/*z* and -1.16 ± 0.44 eV/*z*, respectively, over the 5 s trapping period. The slightly higher uncertainties in mass, charge, and energies compared to the single ion of Figure 2a–b stems from the significant spectral leakage overlap illustrated in red and blue in the single STFT segment (4000–4050 ms) shown in Figure 2d. The relative phase of the ions varies during each segment of the STFT, leading to both constructive and destructive interferences due to spectral leakage overlap over the trapping lifetimes of the ions that result in more variable peak amplitude measurements. The severity of this interference depends on the frequency proximity and the overall signal amplitude. High amplitude, closely spaced signals will have a much larger effect on each other than low amplitude, widely spaced signals. However, the increased measurement errors observed for the ions in Figure 2c–d do not meaningfully affect the mass resolution. The full width at half maximum of the mass distribution measured for the ~100 nm diameter nanoparticle sample used here is ~70 MDa,²⁹ making the small increase in uncertainty originating from small interferences negligible. In general, the analytes most amenable to CDMS analysis are high mass (1 MDa+) and/or have intrinsically high heterogeneity and therefore have sample-based mass resolution limitations.²⁶ Considering that analysis times can be significantly improved by analyzing a larger number of ions simultaneously in each trapping period,^{35,36} the small increase in uncertainty caused by spectral leakage interferences between ions in close frequency proximity is generally acceptable.

Physical Ion-Ion Interactions in Multiplexed CDMS

In addition to ion signal inferences, physical ion-ion interactions can cause changes in ion energy that manifest as changes in ion frequency. SIMION simulations performed by Botamanenko and Jarrold have explored these physical ion-ion interactions and showed that when two ions come near each other, energy transfer can occur, perturbing both the overall energy and trajectory of both interacting ions.³⁷ Proximity in frequency as well as the charge of the ions were predicted to affect the probability of ion-ion interactions.³⁷ However, no ion-ion interactions in CDMS experiments have been previously reported or characterized experimentally.

Figure 3a shows the STFT traces of two ~100 nm nanoparticle ions that undergo physical interaction. As predicted by simulations³⁷ and eq. 1, physical interactions that transfer energy between ions leads to frequency shifts in the observed signals. Frequency increases correspond to decreased ion energy (assuming constant charge and mass) and decreases in frequency indicate increased energy along the main axis of motion in the trap. The

two ions of Figure 3a are initially separated by ~230 Hz and slight perturbations in the frequencies of both ion signal traces appear to be correlated throughout the first 3.51 s of the trapping period, suggesting the two ions are interacting to a minimal extent. At 3.51 s into the trapping period, indicated by the white arrows in Figure 3a, the two ions undergo relatively large (~30 Hz) shifts in frequency in opposite directions, indicating that a large energy transfer between the two ions took place. This time-correlated behavior serves as a signature for physical ion-ion interactions and differentiates interactions from charge emission events where trapped ions only exhibit downward frequency shifts and are uncorrelated with frequency changes in other simultaneously trapped ions.⁴⁰

The ability to time-resolve the interaction of the data in Figure 3a is limited by the 50 ms STFT segment length used. Figure 3b shows the same data analyzed using a much shorter 10 ms STFT segment length to improve time resolution and the time axis is expanded so that the individual FT segment “slices” of the STFT near the interaction can be clearly seen. Using this shorter time segment size necessarily comes at the cost of increasing the widths of the ion frequency traces, but both traces and the frequency change due to the interaction remain sufficiently distinct. Figure 3b shows that the frequency shifts due to the interaction (indicated again by white arrows), occur in less than a single 10 ms segment. This short interaction timescale is consistent with the interactions predicted by simulations of multiple ions oscillating in an electrostatic ion trap.³⁷

Because the ions remain trapped after interacting, ion energies measured before and after the interaction can be separated and fit independently. The energy change for each ion that is attributable to the interaction event can then be measured by finding the difference between the energies before and after the time of the interaction at 3.51 s. This ion-ion interaction resulted in an energy change of $+3.5 \pm 1.1$ eV/z (2840 ± 890 eV total) for the lower frequency ion and a change of -3.0 ± 0.5 eV/z (2580 ± 430 eV total) for the higher frequency ion. The opposite sign and statistically equivalent magnitude of these energy changes indicate that energy is conserved between the two ions within the measurement error; however, it should be noted that measured energies need not be strictly conserved. Deflections that transfer ion energy into the plane perpendicular to the axis of motion will decrease the apparent total energy of the system because only the energy along the main axis of motion is measured. The conservation of energy in this interaction indicates that the energy transfer happens between ions moving in the same direction where the higher velocity ion “pushes” the lower velocity ion along the main axis of motion. This interaction could take place in the field free region, or more likely, in the cone electrodes where the ion velocities are reduced (and ultimately reversed as they turn around) thereby allowing a longer interaction period.

If only energy transfer occurs during physical ion-ion interactions, the masses and charges of the two ions can still be measured and averaged over the entire trapping period because changes in ion energy are accounted for dynamically. To verify that no change in mass or charge occurred as a consequence of the interaction event, these values were determined independently from the data before and after the interaction. The lower frequency ion has a mass of 320.0 ± 1.2 MDa and 320.1 ± 3.0 MDa and a charge of 810.9 ± 1.8 e and 809.0 ± 3.0 e before and after the event, respectively. The higher frequency ion has a mass of

328.9 ± 0.9 MDa and 330.5 ± 1.0 MDa and a charge of 860.2 ± 1.3 *e* and 862.0 ± 1.7 *e* before and after the event, respectively. For both ions, the mass and charge are statistically indistinguishable before and after the interaction, indicating that the frequency change is solely due to energy transfer between the two ions and not fragmentation. Moreover, because only the ion energy changes significantly as a consequence of the interaction, the masses and charge before and after the event can be averaged to decrease the uncertainties in the mass and charge measurements. This yields masses of 320.1 ± 0.9 MDa and 329.4 ± 0.5 MDa and charges of 810.3 ± 1.1 *e* and 860.7 ± 0.7 *e* for the lower and higher frequency ions, respectively. The uncertainties for these interacting ions obtained by signal averaging over the entire trapping period are comparable to those measured for the non-physically interacting ions shown in Figures 2C–D. This is consistent with the similar frequency proximity and associated spectral leakage interferences between the two pairs of ions. It is worth noting that in previous CDMS work, a 100 ms trapping period was sufficient to characterize ~100 nm nanoparticle samples at a resolution determined by the sample heterogeneity and not the instrument resolution.²⁹ In general, CDMS data for this type of sample would be typically acquired using a significantly shorter trapping period. On timescales shorter than 3.51 s, the ions considered here would appear as non-interacting. Significantly longer trap times were used in this work to improve the probability of observing these relatively rare ion-ion interactions.

The ion traces of Figure 1 are a much more typical case for smaller ions like the TMV disk multimers that have less than ~150 *e*, with >95% of trapping events containing multiple ions exhibiting no interactions over the 7.5 s trapping period used for measurements of these TMV ions. However, interactions do occasionally occur even for smaller ions that have fewer charges. The STFT plot shown in Figure 4a shows two ion traces that persist for the full 7.5 s trapping period and have multiple, correlated frequency shifts that indicate significant energy transfer between the ions occurred. It is worth noting that five additional ions were simultaneously trapped, but did not experience any frequency shifts characteristic of interactions. For the two ions shown in Figure 4a, the four most prominent interactions are indicated by the white arrows labeled I-IV and divide the ion traces into five distinct periods (labeled A-E). While interactions II-IV are similar to the interaction in Figure 3b and occur within a short time period (<10 ms), interaction I persists for a relatively long period of time, lasting ~200 ms and appears to be a continuous change, even when the shortest (10 ms) time resolution possible without trace coalescence was used (data not shown). Interactions occurring over this length of time were not predicted by simulations and indicate that physical interactions of multiple types can occur in CDMS.

As was the case for the interacting nanoparticle ions shown in Figure 3, the energy transfer between these two TMV ions can be determined for each interaction event. Because these ions have lower charge and interact more frequently, fits of the energy data for each of the intervening periods (A-E) between interactions have high variability. Thus, instead of using fits of the energy data, average values for each period were determined. A plot of the average energies and corresponding error bars for each of the five periods A-E are shown in Figure 4b. While the transfer of energy is statistically uncertain between some periods because of the higher uncertainties, Figure 4b demonstrates that the changes in energy measured for these ions holistically across all interaction events are closely correlated and significant. In

these correlated events, energy transfers in either direction can occur. The lower frequency ion (blue) gains energy in interactions I, II, and IV, but loses energy in interaction III, with the higher frequency ion (red) exhibiting the opposite energy changes. The less typical behavior of interaction III is likely due to the higher frequency ion being “pushed” by the lower frequency ion further up into the cone potential near the turnaround point.

Taking the difference between periods A and E to quantify the total energy change for the two ions yields an energy change of $+3.7 \pm 2.5$ eV/z for the lower frequency ion while the higher frequency ion energy changes by -7.0 eV/z ± 1.6 . It is possible that energy is conserved along the axis of ion motion for these two ions within the measurement error, but the net energy loss of the system is consistent with a small fraction of the energy lost to the plane perpendicular to the main axis of ion motion and to collisions with background gas. As demonstrated in previous work^{32,39,42} and for the non-interacting ions of Figures 1 and 2, ions trapped in CDMS undergo collisions with background gas that slowly reduce ion energies. Both ion traces in Figure 4a exhibit slow frequency increases in the periods between interaction events, consistent with this energy loss mechanism.

The masses of the two TMV ions in Figure 4 can still be measured with precision comparable to the non-interacting TMV ions of Figure 1. The lower and higher frequency ions have masses of 2.835 ± 0.010 MDa and 2.983 ± 0.010 MDa and charges of 124.0 ± 0.35 *e* and 132.7 ± 0.39 *e*, respectively. The uncertainties for these ions are slightly higher than those measured for the non-physically interacting ions TMV ions shown in Figure 1. This increase in uncertainty is almost certainly a consequence of the closer proximity of the two ion signals in Figure 4 and the resultant spectral leakage overlap, similar to the example given in Figure 2. Thus, even when multiple physical interactions occur, they have very little effect on CDMS measurements of ion mass and charge when using dynamic measurements of ion energy. It has been suggested previously that trapping many ions simultaneously should be avoided because ion-ion interactions will reduce measurement quality due to the greater implied uncertainty in ion energies.^{24,37} While this is true for energy-filter based CDMS measurements, the example shown here using dynamic energy measurements demonstrates that this problem can be easily circumvented. Dynamic energy measurements also eliminate the need for ion energy filtering optics that necessarily reduce ion current and measurement sensitivity. Moreover, because the time required for CDMS analysis can be significantly decreased by analyzing many ions simultaneously, there is a substantial advantage to highly multiplexed measurements.^{35,36}

A “Worst Case” Scenario in Multiplexed CDMS

There are occasional events where signal interferences, direct signal overlap, and physical interactions occur between ions during a single trapping period and significantly affect the analysis of the individual ions. The STFT traces of two ~45 nm nanoparticle ions that are initially separated by ~50 Hz are shown in Figure 5. While the ions are initially distinguishable during the first 1.08 s of the trapping period, their close frequency proximity results in significant spectral leakage interference, but the mass and charge of each ion can still be determined with reasonable precision. The lower and higher frequency ions have masses of 31.0 ± 0.6 MDa and 28.4 ± 0.6 MDa and charges of 264.4 ± 2.4 *e* and $251.2 \pm$

2.6 e , respectively. In typical CDMS experiments, ions are trapped for 1 s or less.^{26,34} In that case, this spectral interference would just lead to a slightly higher uncertainty in the mass and charge measurements. At 1.08 s, an energy transfer event occurs, which results in the two ions having nearly identical frequencies in the period from 1.08 s to 2.25 s. Because the ion frequencies are overlapping, they can constructively or destructively interfere with each other depending on their relative phases, leading to the irregular frequency beat pattern observed during this period. No mass or charge information can be extracted from this period. Typically, if overlap is observed during the trapping period, the involved ions are discarded to simplify processing of the CDMS data that occurs concurrently with data acquisition.³⁵ However, in this case, another physical interaction at 2.25 s causes the ion signals to separate into two distinct ion frequencies differing by ~ 70 Hz. The period of overlap effectively scrambles the identity of original ion signals and the two new frequencies cannot be assigned to the original ions using the STFT plot. However, the masses and charges measured for the two ions during the period from 2.25 s to the end of the trapping period (5 s), makes it possible to identify both ions before and after signal overlap. The new lower frequency ion has a mass of 30.6 ± 0.2 MDa and a charge of $262.5 \pm 1.2 e$, matching that of the original lower frequency ion. Similarly, the new higher frequency ion has a mass of 29.1 ± 0.5 MDa and a charge of $249.6 \pm 2.3 e$, matching the original higher frequency ion. At 3.16 s, another large physical interaction occurs, with the low frequency ion gaining $+2.9 \pm 2.3$ eV/ z and the high frequency ion losing -6.4 ± 2.4 eV/ z , based on average energies measured before and after this interaction. As was the case for the ions of Figures 3 and 4, energy is statistically conserved in this interaction, but the net energy loss suggests energy transfer to the plane perpendicular to the measurement axis and/or energy losses due to background gas collision occurred. Overall, this example demonstrates that useful mass, charge, and ion-ion interaction information can be extracted even when both significant ion signal interferences and large physical ion-ion interactions occur.

Conclusions

Physical ion-ion interactions have been experimentally observed for the first time in CDMS. These interactions are relatively rare events because the ions are initially distributed throughout the trap and there is no phase coherence even for ions with the exact same m/z . Physical interactions are more likely when two ions have similar frequencies, are highly charged, and are trapped for long periods of time. In the case of a filter-based CDMS instrument that assumes a constant energy throughout the entire measurement, these physical interactions scramble the original energies of the involved ions and, like signal analysis-based interferences, degrade measurement quality. However, unlike signal interferences, physical interactions do not significantly affect the mass measurement precision when the dynamic energy measurement method is used. Ion energies and frequencies can be precisely measured before and after the interaction, and any changes are accounted for in the determination of ion m/z such that no additional uncertainty is incurred. The change in energy before and after physical interaction events can also be quantified using the dynamic CDMS energy measurement method. In the examples in this work, energy changes for the two interacting ions are correlated, *i.e.*, if one ion gains energy, the other ion loses energy. While not a strict requirement due to the possibility of energy transfer into vectors

perpendicular to the axis of ion motion and energy losses to background gas, this work shows that energy transfer resulting from ion-ion interactions tends to be largely conserved in the main axis of ion motion within the electrostatic ion trap.

For large MDa-sized molecules, the heterogeneity of the sample being characterized is often sufficiently high that instrumental measurement precision is not the limiting factor in the resolution of the resultant mass histogram. This work shows that signal interferences can marginally increase measurement uncertainties, but in most cases, this slight reduction in performance will have little to no effect on the overall mass distribution measured for a sample of MDa-sized molecules. Moreover, physical interactions that change ion energies can be wholly accounted for using dynamic energy analysis. Thus, it is typically advisable to prioritize multiplexing and gains in acquisition speed for these types of samples.

Signal interferences and physical ion-ion interactions both have notable signatures in multiplexed CDMS data. Signal interferences, such as spectral leakage overlap or direct frequency overlap, can degrade the ability to make some individual ion measurements in CDMS when multiple ions are present. Careful choice of signal analysis and tracing parameters can be used to either reduce measurement uncertainties or prioritize multiplexing and analysis speed. However, there will always be a tradeoff in the choice of signal analysis parameters used. A way to improve CDMS performance irrespective of the signal analysis is to increase the frequency space over which ion signals are spread. Using this strategy decreases the probability of ion interferences and allows either higher performance or a greater extent of multiplexing. One way this can be accomplished in CDMS is by broadening the energy bandwidth of ions admitted into the electrostatic ion trap. This strategy is incompatible with filter-based energy measurements but is ideally suited to the dynamic method used in this work.

Acknowledgements

The authors are grateful for financial support from the National Institutes of Health (5R01GM139338) and the Arnold and Mabel Beckman Foundation Postdoctoral Fellowship in Chemical Instrumentation (C.C.H.). The authors thank Dr. Amanda J. Bischoff and Professor Matthew B. Francis for supplying the four TMV disk stack ions shown in this work.

References

- (1). Vedel F; André J Influence of Space Charge on the Computed Statistical Properties of Stored Ions Cooled by a Buffer Gas in a Quadrupole Rf Trap. *Phys. Rev. A* 1984, 29 (4), 2098–2101.
- (2). Cox KA; Cleven CD; Cooks RG Mass Shifts and Local Space Charge Effects Observed in the Quadrupole Ion Trap at Higher Resolution. *Int. J. Mass Spectrom. Ion Process* 1995, 144 (1–2), 47–65.
- (3). Hager JW A New Linear Ion Trap Mass Spectrometer. *Rapid Commun. Mass Spectrom* 2002, 16 (6), 512–526.
- (4). Jeffries JB; Barlow SE; Dunn GH Theory of Space-Charge Shift of Ion Cyclotron Resonance Frequencies. *Int. J. Mass Spectrom. Ion Process* 1983, 54 (1–2), 169–187.
- (5). Ledford EB; Rempel DL; Gross ML Space Charge Effects in Fourier Transform Mass Spectrometry. *Mass Calibration. Anal. Chem* 1984, 56 (14), 2744–2748. [PubMed: 6524653]
- (6). Easterling ML; Mize TH; Amster IJ Routine Part-per-Million Mass Accuracy for High-Mass Ions: Space-Charge Effects in MALDI FT-ICR. *Anal. Chem* 1999, 71 (3), 624–632. [PubMed: 21662720]

- (7). Xiang X; Grosshans PB; Marshall AG Image Charge-Induced Ion Cyclotron Orbital Frequency Shift for Orthorhombic and Cylindrical FT-ICR Ion Traps. *Int. J. Mass Spectrom. Ion Process* 1993, 125 (1), 33–43.
- (8). Gorshkov MV; Good DM; Lyutvinskiy Y; Yang H; Zubarev RA Calibration Function for the Orbitrap FTMS Accounting for the Space Charge Effect. *J. Am. Soc. Mass Spectrom* 2010, 21 (11), 1846–1851. [PubMed: 20696596]
- (9). Kharchenko A; Vladimirov G; Heeren RMA; Nikolaev EN Performance of Orbitrap Mass Analyzer at Various Space Charge and Non-Ideal Field Conditions: Simulation Approach. *J. Am. Soc. Mass Spectrom* 2012, 23 (5), 977–987. [PubMed: 22354683]
- (10). Grinfeld D; Stewart H; Skoblin M; Denisov E; Monastyrsky M; Makarov A Space-Charge Dynamics in Orbitrap Mass Spectrometers. *Int. J. Mod. Phys. A* 2019, 34 (36), 1942007.
- (11). Gorshkov MV; Fornelli L; Tsybin YO Observation of Ion Coalescence in Orbitrap Fourier Transform Mass Spectrometry. *Rapid Commun. Mass Spectrom* 2012, 26 (15), 1711–1717. [PubMed: 22730091]
- (12). Marshall AG; Hendrickson CL; Jackson GS Fourier Transform Ion Cyclotron Resonance Mass Spectrometry: A Primer. *Mass Spectrom. Rev* 1998, 17 (1), 1–35. [PubMed: 9768511]
- (13). Zubarev RA; Makarov A Orbitrap Mass Spectrometry. *Anal. Chem* 2013, 85 (11), 5288–5296. [PubMed: 23590404]
- (14). Bruce JE; Cheng X; Bakhtiar R; Wu Q; Hofstadler SA; Anderson GA; Smith RD Trapping, Detection, and Mass Measurement of Individual Ions in a Fourier Transform Ion Cyclotron Resonance Mass Spectrometer. *J. Am. Chem. Soc* 1994, 116 (17), 7839–7847.
- (15). Bruce JE; Anderson GA; Udseth HR; Smith RD Large Molecule Characterization Based upon Individual Ion Detection with Electrospray Ionization-FTICR Mass Spectrometry. *Anal. Chem* 1998, 70 (3), 519–525. [PubMed: 21644751]
- (16). Cheng X; Bakhtiar R; Van Orden S; Smith RD Charge-State Shifting of Individual Multiply-Charged Ions of Bovine Albumin Dimer and Molecular Weight Determination Using an Individual-Ion Approach. *Anal. Chem* 1994, 66 (13), 2084–2087. [PubMed: 8067525]
- (17). Makarov A; Denisov E Dynamics of Ions of Intact Proteins in the Orbitrap Mass Analyzer. *J. Am. Soc. Mass Spectrom* 2009, 20 (8), 1486–1495. [PubMed: 19427230]
- (18). Kafader JO; Melani RD; Senko MW; Makarov AA; Kelleher NL; Compton PD Measurement of Individual Ions Sharply Increases the Resolution of Orbitrap Mass Spectra of Proteins. *Anal. Chem* 2019, 91 (4), 2776–2783. [PubMed: 30609364]
- (19). Wörner TP; Snijder J; Bennett A; Agbandje-McKenna M; Makarov AA; Heck AJR Resolving Heterogeneous Macromolecular Assemblies by Orbitrap-Based Single-Particle Charge Detection Mass Spectrometry. *Nat. Methods* 2020, 17 (4), 395–398. [PubMed: 32152501]
- (20). Kafader JO; Beu SC; Early BP; Melani RD; Durbin KR; Zabrouskov V; Makarov AA; Maze JT; Shinholt DL; Yip PF; Kelleher NL; Compton PD; Senko MW STORI Plots Enable Accurate Tracking of Individual Ion Signals. *J. Am. Soc. Mass Spectrom* 2019, 30 (11), 2200–2203. [PubMed: 31512223]
- (21). Wörner TP; Aizikov K; Snijder J; Fort KL; Makarov AA; Heck AJR Frequency Chasing of Individual Megadalton Ions in an Orbitrap Analyser Improves Precision of Analysis in Single-Molecule Mass Spectrometry. *Nat. Chem* 2022, 14 (5), 515–522. [PubMed: 35273389]
- (22). Weinheimer AJ The Charge Induced on a Conducting Cylinder by a Point Charge and Its Application to the Measurement of Charge on Precipitation. *J. Atmos. Ocean. Technol* 1988, 5 (2), 298–304.
- (23). Gustafson EL; Murray HV; Caldwell T; Austin DE Accurately Mapping Image Charge and Calibrating Ion Velocity in Charge Detection Mass Spectrometry. *J. Am. Soc. Mass Spectrom* 2020, 31 (10), 2161–2170. [PubMed: 32856905]
- (24). Keifer DZ; Pierson EE; Jarrold MF Charge Detection Mass Spectrometry: Weighing Heavier Things. *Analyst* 2017, 142 (10), 1654–1671. [PubMed: 28443838]
- (25). Elliott AG; Merenbloom SI; Chakrabarty S; Williams ER Single Particle Analyzer of Mass: A Charge Detection Mass Spectrometer with a Multi-Detector Electrostatic Ion Trap. *Int. J. Mass Spectrom* 2017, 414, 45–55. [PubMed: 29129967]

- (26). Harper CC; Miller ZM; Lee H; Bischoff AJ; Francis MB; Schaffer DV; Williams ER Effects of Molecular Size on Resolution in Charge Detection Mass Spectrometry. *Anal. Chem* 2022, 94 (33), 11703–11712. [PubMed: 35961005]
- (27). Keifer DZ; Shinholt DL; Jarrold MF Charge Detection Mass Spectrometry with Almost Perfect Charge Accuracy. *Anal. Chem* 2015, 87 (20), 10330–10337. [PubMed: 26418830]
- (28). Hogan JA; Jarrold MF Optimized Electrostatic Linear Ion Trap for Charge Detection Mass Spectrometry. *J. Am. Soc. Mass Spectrom* 2018, 29 (10), 2086–2095. [PubMed: 29987663]
- (29). Harper CC; Miller ZM; McPartlan MS; Jordan JS; Pedder RE; Williams ER Accurate Sizing of Nanoparticles Using a High-Throughput Charge Detection Mass Spectrometer without Energy Selection. *ACS Nano* 2023, 17 (8), 7765–7774. [PubMed: 37027782]
- (30). Miller ZM; Harper CC; Lee H; Bischoff AJ; Francis MB; Schaffer DV; Williams ER Apodization Specific Fitting for Improved Resolution, Charge Measurement, and Data Analysis Speed in Charge Detection Mass Spectrometry. *J. Am. Soc. Mass Spectrom* 2022, 33 (11), 2129–2137. [PubMed: 36173188]
- (31). Todd AR; Alexander AW; Jarrold MF Implementation of a Charge-Sensitive Amplifier without a Feedback Resistor for Charge Detection Mass Spectrometry Reduces Noise and Enables Detection of Individual Ions Carrying a Single Charge. *J. Am. Soc. Mass Spectrom* 2020, 31 (1), 146–154. [PubMed: 32881508]
- (32). Harper CC; Elliott AG; Lin HW; Williams ER Determining Energies and Cross Sections of Individual Ions Using Higher-Order Harmonics in Fourier Transform Charge Detection Mass Spectrometry (FT-CDMS). *J. Am. Soc. Mass Spectrom* 2018, 29 (9), 1861–1869. [PubMed: 29860679]
- (33). Elliott AG; Harper CC; Lin HW; Williams ER Effects of Individual Ion Energies on Charge Measurements in Fourier Transform Charge Detection Mass Spectrometry (FT-CDMS). *J. Am. Soc. Mass Spectrom* 2019, 30 (6), 946–955. [PubMed: 30430436]
- (34). Jarrold MF Applications of Charge Detection Mass Spectrometry in Molecular Biology and Biotechnology. *Chem. Rev* 2022, 122 (8), 7415–7441. [PubMed: 34637283]
- (35). Harper CC; Elliott AG; Oltrogge LM; Savage DF; Williams ER Multiplexed Charge Detection Mass Spectrometry for High-Throughput Single Ion Analysis of Large Molecules. *Anal. Chem* 2019, 91 (11), 7458–7468. [PubMed: 31082222]
- (36). Harper CC; Williams ER Enhanced Multiplexing in Fourier Transform Charge Detection Mass Spectrometry by Decoupling Ion Frequency from Mass to Charge Ratio. *J. Am. Soc. Mass Spectrom* 2019, 30 (12), 2637–2645. [PubMed: 31720975]
- (37). Botamanenko DY; Jarrold MF Ion-Ion Interactions in Charge Detection Mass Spectrometry. *J. Am. Soc. Mass Spectrom* 2019, 30 (12), 2741–2749. [PubMed: 31677069]
- (38). Todd AR; Barnes LF; Young K; Zlotnick A; Jarrold MF Higher Resolution Charge Detection Mass Spectrometry. *Anal. Chem* 2020, 92 (16), 11357–11364. [PubMed: 32806905]
- (39). Elliott AG; Harper CC; Lin HW; Williams ER Mass, Mobility and MSN Measurements of Single Ions Using Charge Detection Mass Spectrometry. *Analyst* 2017, 142 (15), 2760–2769. [PubMed: 28636005]
- (40). Harper CC; Brauer DD; Francis MB; Williams ER Direct Observation of Ion Emission from Charged Aqueous Nanodrops: Effects on Gaseous Macromolecular Charging. *Chem. Sci* 2021, 12 (14), 5185–5195. [PubMed: 34168773]
- (41). Hanozin E; Harper CC; McPartlan MS; Williams ER Dynamics of Rayleigh Fission Processes in ~100 Nm Charged Aqueous Nanodrops. *ACS Cent. Sci* 2023.
- (42). Elliott AG; Harper CC; Lin HW; Susa AC; Xia Z; Williams ER Simultaneous Measurements of Mass and Collisional Cross-Section of Single Ions with Charge Detection Mass Spectrometry. *Anal. Chem* 2017, 89 (14), 7701–7708. [PubMed: 28621517]
- (43). Bischoff AJ; Harper CC; Williams ER; Francis MB Characterizing Heterogeneous Mixtures of Assembled States of the Tobacco Mosaic Virus Using Charge Detection Mass Spectrometry. *J. Am. Chem. Soc* 2022, 144 (51), 23368–23378. [PubMed: 36525679]
- (44). Ramsey AV; Bischoff AJ; Francis MB Enzyme Activated Gold Nanoparticles for Versatile Site-Selective Bioconjugation. *J. Am. Chem. Soc* 2021, 143 (19), 7342–7350. [PubMed: 33939917]

- (45). Contino NC; Pierson EE; Keifer DZ; Jarrold MF Charge Detection Mass Spectrometry with Resolved Charge States. *J. Am. Soc. Mass Spectrom* 2013, 24 (1), 101–108. [PubMed: 23197308]
- (46). Harris FJ On the Use of Windows for Harmonic Analysis with the Discrete Fourier Transform. *Proc. IEEE* 1978, 66 (1), 51–83.
- (47). Leach FE; Kharchenko A; Vladimirov G; Aizikov K; O'Connor PB; Nikolaev E; Heeren RMA; Amster IJ Analysis of Phase Dependent Frequency Shifts in Simulated FTMS Transients Using the Filter Diagonalization Method. *Int. J. Mass Spectrom* 2012, 325–327, 19–24.
- (48). Grinfeld D; Aizikov K; Kreutzmann A; Damoc E; Makarov A Phase-Constrained Spectrum Deconvolution for Fourier Transform Mass Spectrometry. *Anal. Chem* 2017, 89 (2), 1202–1211. [PubMed: 27982570]

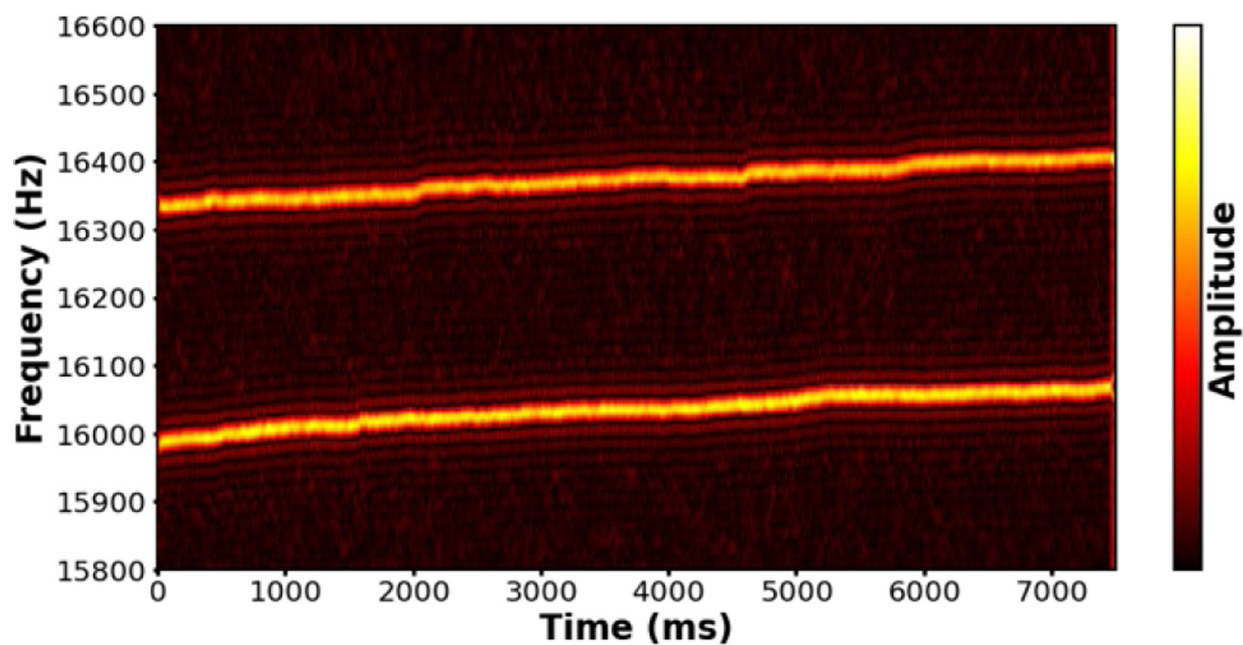


Figure 1. STFT plot of traces for two TMV ions trapped for 7.5 s showing the evolution of the ion frequencies of motion with time. The ion frequencies increase slowly throughout the trapping period due to collisions with background gas, but the ions do not interact or interfere.

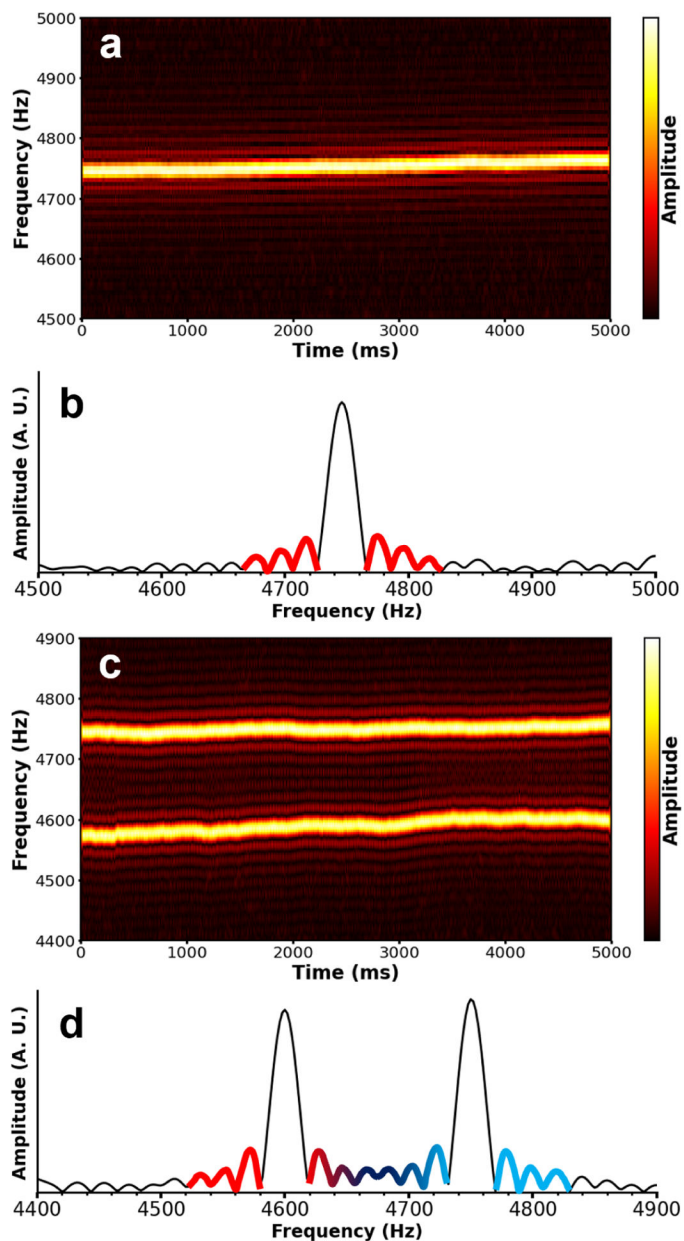


Figure 2.

Ion signals for ~100 nm diameter polystyrene nanoparticles. The STFT plot in (a) shows a single ion trapped for 5 s that shifts slightly in frequency over time due to collisions with background gas. A single segment of the STFT plot (4000–4050 ms) is shown in (b) with spectral leakage artifacts inherent to unapodized FT analyses highlighted in red. The STFT plot in (c) shows the traces of two ions separated by ~170 Hz that do not physically interact. However, a single STFT segment (4000–4050 ms) in (d) shows that the two signals are close enough in frequency space that spectral leakages (red and blue) of the two signals have sufficiently high amplitudes in the vicinity of main signal peaks for interferences to occur.

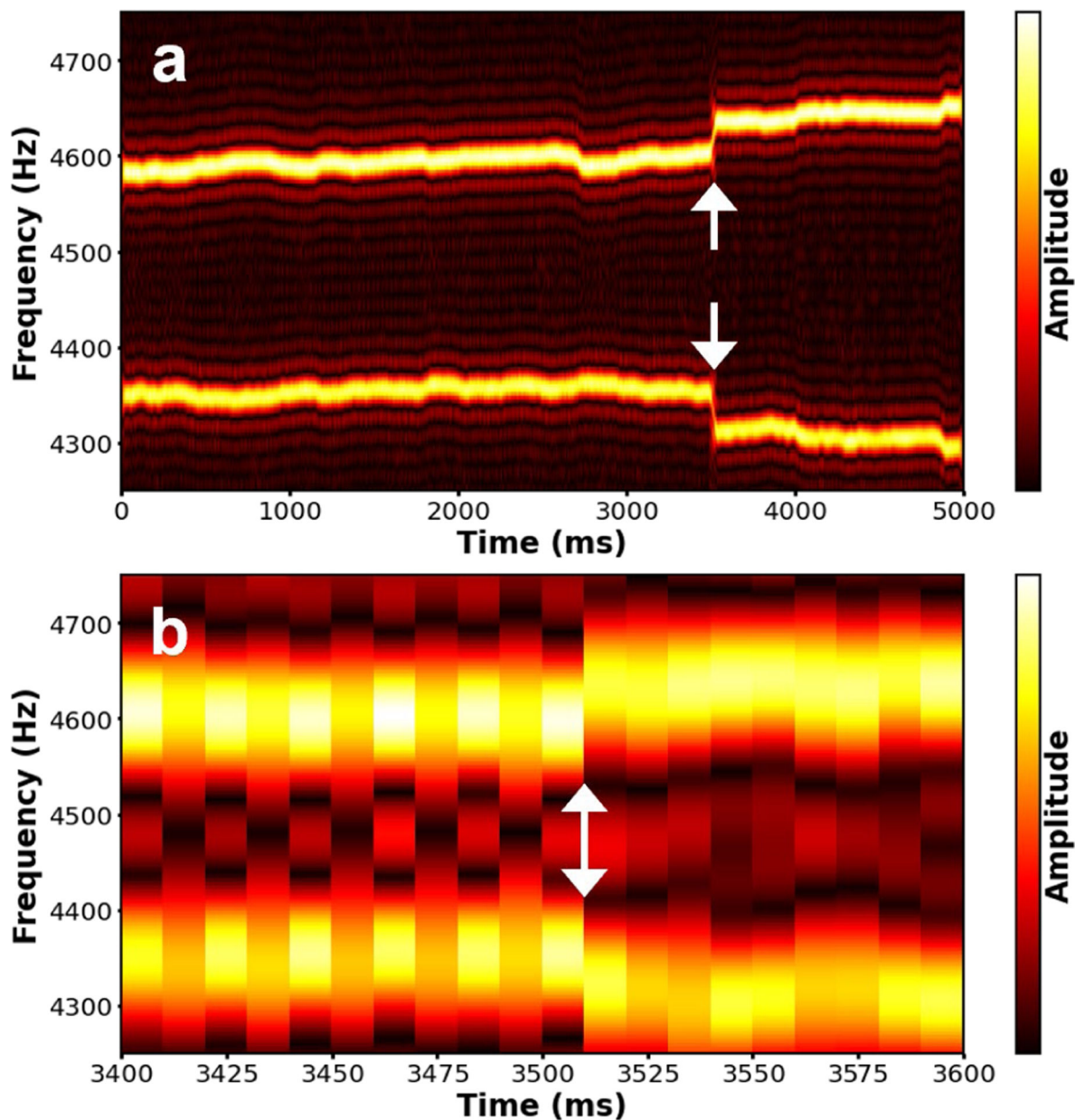


Figure 3. STFT traces for two ~ 100 nm diameter polystyrene nanoparticles that undergo a significant physical ion-ion interaction ~ 3.51 s into the trapping period. The physical ion-ion interaction is indicated by the white arrows and is characterized by ion frequencies shifting ~ 30 Hz in opposite directions. The longer (50 ms) STFT segment size used in (a) allows for accurate frequency and amplitude determinations of the ions before and after the interaction. In (b), the time axis is expanded to show the region between 3400–3600 ms, and a shorter (10 ms) STFT segment size is used to increase time resolution and each 10 ms STFT segment is clearly delineated in (b). The shift in frequency (indicated by white arrows) occurs completely within a single STFT segment, indicating that this interaction lasted less than 10 ms.

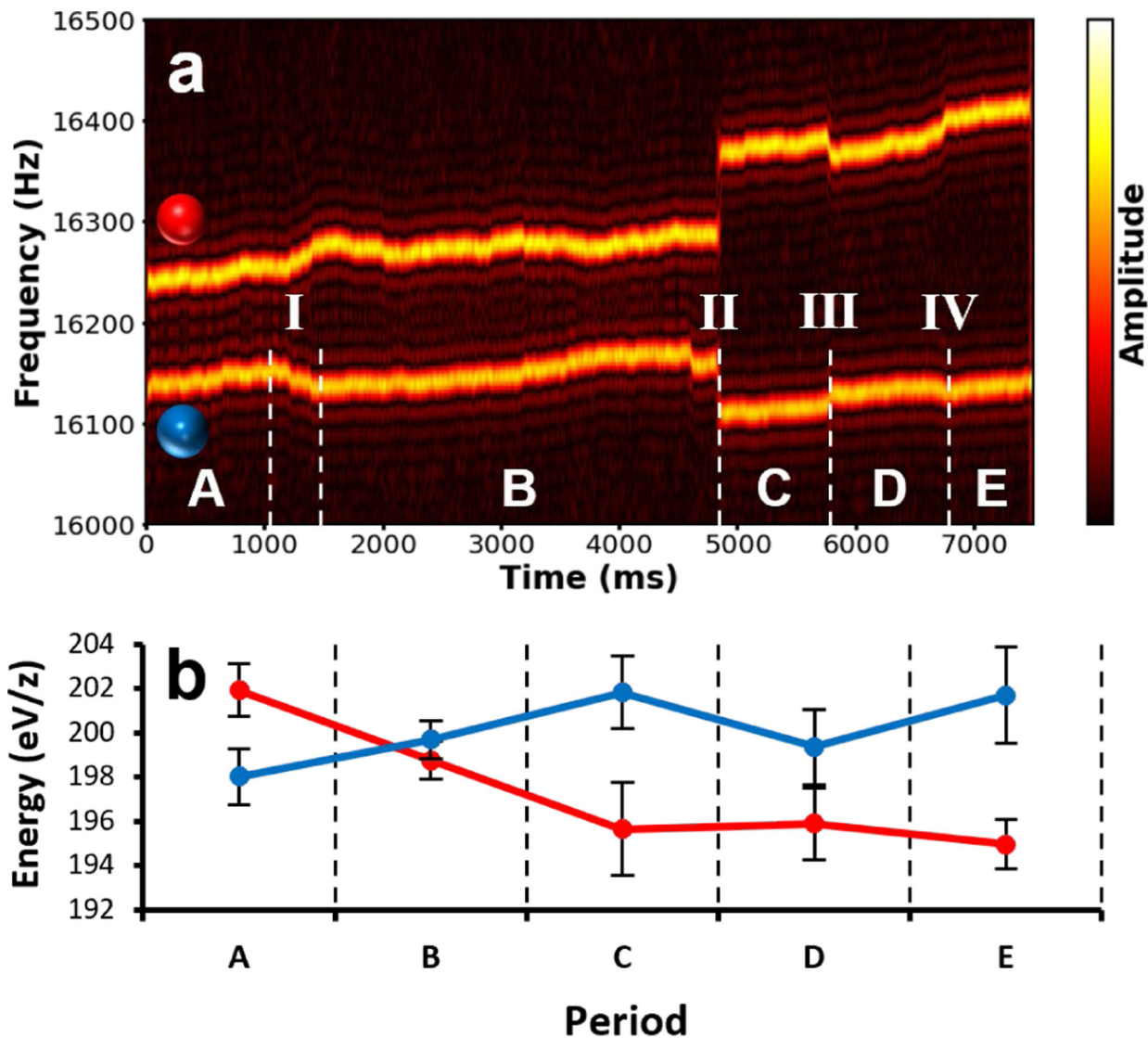


Figure 4. STFT plot (a) and measured average energies between physical interactions (b) for two TMV ions trapped for 7.5 s. The ions undergo four prominent physical interactions (labeled I-IV) over the course of the trapping period, making it possible to divide the trace into five distinct periods (A-E). The average energies measured during each of these periods and their associated uncertainties are shown in (b), with the data in blue corresponding to the lower frequency ion and the data in red corresponding to the higher frequency ion. The changes in energy between each period for each ion have a clear opposing correlation, e.g., when one ion increases in energy, a similar decrease is observed for the other ion.

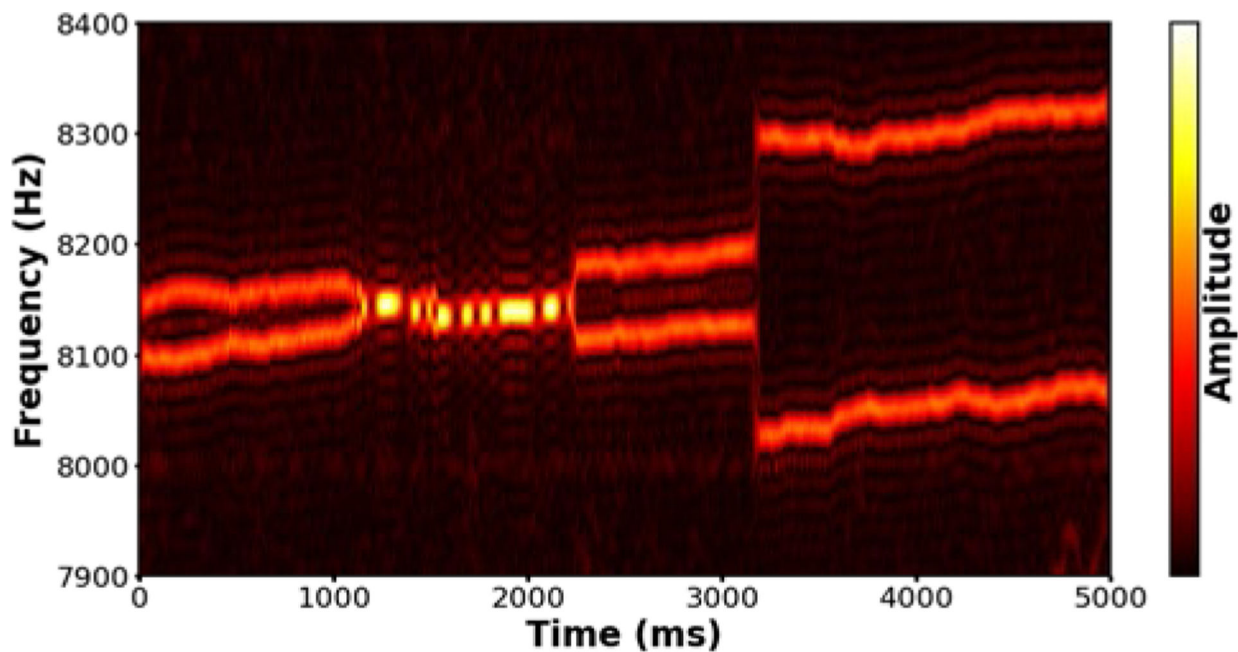


Figure 5.

STFT plot of two ~50 nm diameter polystyrene nanoparticles trapped for 5 s that undergo both physical interactions as well as significant signal interferences. The two ions are distinct until 1.08 s, when a physical interaction results in the two ions overlapping with nearly identical frequencies. This overlap period continues until 2.25 s, when another physical interaction separates the ion frequencies. A final large physical interaction occurs at 3.16 s. While the ion identities are scrambled by period of overlap from 1.08–2.25 s, mass and charge measurements made on the periods where ions are separated indicate that the initial high frequency ion corresponds to higher frequency ion post-overlap and the initial low frequency ion corresponds to the lower frequency ion post-overlap.